An aqueous capacitor battery hybrid device based on Na-ion insertion-deinsertion in λ-MnO$_2$ positive electrode

Ying Zhang, Congli Yuan, Ke Ye, Xue Jiang, Jinling Yin, Guiling Wang, Dianxue Cao *

Key Laboratory of Superlight Materials and Surface Technology of Ministry of Education, College of Materials Science and Chemical Engineering, Harbin Engineering University, Harbin, 150001, PR China

ABSTRACT

A high-performance capacitor battery AC/λ-MnO$_2$ based on Na-ion insertion-deinsertion into λ-MnO$_2$ in 1 mol dm^{-3} Na$_2$SO$_4$ solution is successfully demonstrated. A simple acid leaching technique is used to produce λ-MnO$_2$ by treating LiMn$_2$O$_4$ with H$_2$SO$_4$. X-ray power diffraction and inductively coupled plasma analysis provide supporting evidences for the extraction of Li$^+$ from the LiMn$_2$O$_4$, and the particle morphology of λ-MnO$_2$ is studied by scanning and transmission electron microscopy. A high specific capacity of 390.7 mAh g^{-1} is obtained for the λ-MnO$_2$ electrode at a current density of 13.6 mA g^{-1} with a nearly 100% efficiency. The capacitor battery AC/λ-MnO$_2$ can operate at a cell voltage as high as 2.2 V, and it exhibits a specific energy of 19.7 Wh Kg^{-1} at a high power density of 3500 W Kg^{-1} and a high energy density of 71.7 Wh Kg^{-1} at a low power density of 403 W Kg^{-1}. It has potentials to be used as an energy storage device for the integration of solar and wind power into the electrical power grid.

© 2014 Elsevier Ltd. All rights reserved.

1. Introduction

The broad penetration of solar, wind, micro sterling engines and solid oxide fuel cells and the maturity of electricity grids increase the need for large-scale rechargeable energy storage devices. Secondary batteries and electrochemical capacitors have caught extensive attention because both of them are effective methods for electrochemical energy storage. Secondary batteries are competent for achieving a much higher energy density while electrochemical capacitors can provide an appreciable higher power density and excellent cycling stability [1–6]. Observing the present-day world, the fast deployment of renewable energy sources such as solar and wind power increases the needs for large-scale rechargeable energy storage devices, which are inexpensive, safe, environmental friendly, can respond rapidly, and have long cycle life, high power and high energy efficiency [7]. A hybrid energy storage system called capacitor battery which combines the high energy density of secondary battery and the high power density and long cycle life of supercapacitor can be an attractive candidate of energy storage devices for these renewable energy sources. One electrode of this device is activated carbon (AC) for electrochemical double-layer capacitance (EDLC) and the other is an ion-intercalated compound for battery electrode, such as

PPy-AC/CuHCF [7], AC/Na$_4$Mn$_9$O$_{18}$ [8], AC/LiMn$_2$O$_4$ [9] and AC/MnO$_2$ [10,11]. For the above mentioned devices, the EDLC electrode stores energy through a reversible nonfaradaic process of ionic movement and the battery electrode utilizes a reversible faradic reaction of ion insertion/extraction [12–14]. Such devices using the neutral pH aqueous electrolyte can provide a sufficient energy density, a high ionic conductivity and they are green, low-cost, safe and environmentally friendly, which would be most appealing for manufacturing and large-scale systems from the cost and environment perspectives. However, an obvious demerit of aqueous electrolytes is the narrow electrochemical window, which can result in low energy density. The operational voltage of PPy-AC/CuHCF, AC/Na$_4$Mn$_9$O$_{18}$, AC/LiMn$_2$O$_4$ and AC/MnO$_2$ is all less than 2 V.

The key to achieve a high performance in aqueous electrolyte is through developing adaptive electrode materials. Manganese dioxide is a widely-used material in electrochemical cells for its abundant and benign. Due to the different interlink of the octahedral MnO$_6$ moiety, α, β, γ, δ and λ forms of MnO$_2$ are classified into three groups according to the tunnel structures in one, two or three dimensions [15], of which the α, β and γ forms are 1D tunnels, the δ and λ is 2D layered compound and 3D spinel structure, respectively [16]. The properties of MnO$_2$ largely depend on its crystal structure [17,18]. Because of the diverse structures, MnO$_2$ has been widely used as the electrode material in batteries [16] as well as in supercapacitors [19–25]. Asymmetric supercapacitor AC/MnO$_2$ has been widely investigated. But most of them

used amorphous MnO_2 as electrode material and the cycling performance was not good enough in the presence of dissolved oxygen [26–28]. The treatment of $LiMn_2O_4$ with dilute acid solution yields an allotrope of MnO_2, denoted as λ-MnO_2. In the spinel $LiMn_2O_4$, octahedral MnO_6 forms a cubic structure with Li^+ in the tetrahedral $8a$ sites and Mn^{3+} and Mn^{4+} occupying the octahedral $16d$ sites [29]. The insertion and deinsertion of Li ion in the 3D network structure of Mn_2O_4 occur via the gap of adjacent tetrahedral and octahedral along the channel of $8a$-$16c$-$8a$, which is the theoretical basis of $LiMn_2O_4$ used as the material of secondary lithium battery. After the acid treatment, $LiMn_2O_4$ maintains the spinel framework but with empty $8a$ sites, resulting in a unique open structure for ions to intercalate and deintercalate.

Here we demonstrate a facile approach for synthesizing nanoscale MnO_2 that used the available and traditional commercialized material $LiMn_2O_4$ by acid leaching method for an aqueous capacitor battery. In this paper, we studied a new Na-ion capacitor battery in 1 mol dm^{-3} Na_2SO_4 neutral system using λ-MnO_2 as an intercalation battery electrode and AC as a capacitor electrode. We demonstrated that λ-MnO_2 has a large specific capacity for the intercalation of Na-ion in an aqueous system. The AC/λ-MnO_2 capacitor battery has an operational voltage higher than any other aqueous system reported and it exhibits a high energy density even at a high power density. We believe this kind of energy device will be appealing for large-scale commercial production because it combines the superiorities of secondary batteries and electrochemical capacitors, and the utilization of abundant and benign Mn and aqueous electrolyte decreases the cost.

2. Experimental

2.1. Preparation of λ-MnO_2

The λ-MnO_2 powder was synthesized by removing lithium from $LiMn_2O_4$ (purchased from Wu Jie Science & Technology Co., Ltd.) via H_2SO_4 acid leaching [30]. The effects of acid concentrations (0.28, 0.56, 1.68, and 2.24 mol dm^{-3}), leaching temperatures (30, 50, 80, and 100 °C) and leaching time (3, 6, 12, and 24 h) on the Na-ion insertion/deinsertion into λ-MnO_2 were systemically investigated, and the optimum leaching condition was found to be: H_2SO_4 is 0.56 mol dm^{-3}, the temperature is 50 °C, and the leaching time is 12 h. So the λ-MnO_2 sample reported in this paper was prepared by stirring a suspension of about 5 mg $LiMn_2O_4$ in 100 cm^{-3} 0.56 mol dm^{-3} H_2SO_4 at 50 °C for 12 h. The amaranthine solution was then decanted, filtered, ultrasonic-cleaned for 4 hours and washed several times with deionized water. The resulting powder was dried at 60 °C in air for 1 h and then in 100 °C vacuum oven for 12 h. The detailed information for experimental parameter optimization has been described in the Supporting Information.

The structure of λ-MnO_2 was analyzed by X-ray diffractometer (XRD Rigaku TTR III) with Cu $K\alpha$ radiation (λ=0.154178 nm). The 2θ ranges from 10° to 75° with a scan rate of 5° min^{-1}, and a step with 0.01°. The degree of lithium leaching was measured by using an inductively coupled plasma atomic emission spectrometer (ICP, Xseries II, Thermo Scientific). Scanning electron microscope (SEM) and transmission electron microscope (TEM) pictures were obtained with a JEOL JSM-6480 microscope and a FEI Teccai G2 S-Twin microscope, respectively.

2.2. Electrochemical measurement of the λ-MnO_2 electrode and the AC/λ-MnO_2 capacitor battery

The λ-MnO_2 positive electrode was prepared by mixing 80 wt. % of λ-MnO_2 powder, 10 wt. % acetylene black and 10 wt. % polyvinylidene difluoride (PVDF) binder in N-methyl-2-pyrrolidone (NMP). The obtained thick paste was coated onto 1.0 cm × 1.0 cm carbon fiber cloths (CFC) and dried in 100 °C vacuum oven. The loading of λ-MnO_2 in the electrode is 5 mg cm^{-2}. The AC electrode was prepared in the same way with an AC loading of 10 mg cm^{-2}. Single electrode test was carried in a three-electrode system. A graphite sheet and a saturated calomel electrode (SCE) were used as the counter and reference electrode, respectively. All potentials were reported vs. SCE in this work. λ-MnO_2 electrode acted as the working electrode. The electrolyte was 1 mol dm^{-3} Na_2SO_4 aqueous solution. The cyclic voltammetry (CV) and electrochemical impedance spectroscopy (EIS) were performed using a computerized potentiostat (Autolab PGSTAT 302, Eco Chemie). Galvanostatic charge and discharge tests were carried on a LAND Battery Tester (model CT2001A, Newware, China). As showed the device drawing in Fig. 1, the AC/λ-MnO_2 capacitor battery was fabricated by holding the λ-MnO_2 electrode, a filter paper and the AC electrode sandwich together using two titanium frames on each side, which also acted as the electrode tabs. The sandwich was immersed in 1 mol dm^{-3} Na_2SO_4 solution, which was bubbled by N_2 gas for 30 min to eliminate oxygen before tests [26].

3. Results and Discussion

3.1. Characterization of the λ-MnO_2

The X-ray powder diffraction patterns of $LiMn_2O_4$ and λ-MnO_2 were compared in Fig. 2. The diffraction peaks of $LiMn_2O_4$ matched well with the pure cubic spinel structure (JCPDS: 54-0252). Powder X-ray diffraction of λ-MnO_2 verified the formation of lambda manganese dioxide (JCPDS: 44-0992), which retained the spinel structure after the delithiation from $LiMn_2O_4$. The relative intensity of the (400) reflection was higher than that of the (311) reflection for $LiMn_2O_4$. While the relative intensity of the (400) reflection was equal to that of the (311) reflection for λ-MnO_2. This was an indication of the disproportionation of Mn^{3+} to Mn^{4+} and Mn^{2+} in $LiMn_2O_4$ [30]. All diffraction peaks of λ-MnO_2 broaden slightly and showed a shift of 2θ towards higher values. This was because that the interplanar spacing became smaller after the extraction of Li from the $LiMn_2O_4$. Also, the lattice parameter of λ-MnO_2 (a = 0.804 nm) was smaller than that of $LiMn_2O_4$ (a = 0.823 nm), indicating a slightly contraction of the crystal cell.

ICP-AES datas for the raw material $LiMn_2O_4$ and the λ-MnO_2 sample showed that the lithium content was significantly reduced by acid treatment, as for $Li_xMn_2O_4$, x had changed from 1 to 0.027. After the extraction of lithium from the $LiMn_2O_4$, the presence of amaranthine solution in the filtrate suggested that part manganese ions had changed into Mn^{2+}. A significant decrease in the sample mass from 5 g $LiMn_2O_4$ to 3 g λ-MnO_2 also confirmed the
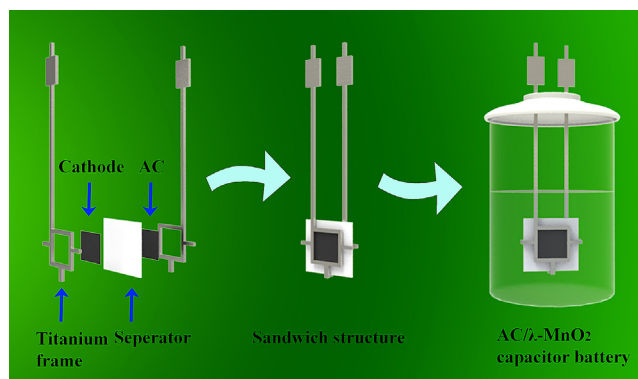

Fig. 1. The assembling process of AC/λ-MnO_2 capacitor battery.